

THE INFLUENCE OF INTERSHELL INTERACTION ON  
THE 3d AND 5d BRANCHING RATIO OF Cu AND Au

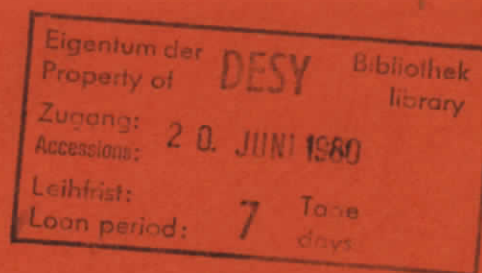
by

J. Barth, R. Bruhn and B. Sonntag

*II. Institut für Experimentalphysik der Universität Hamburg  
and  
Deutsches Elektronen-Synchrotron DESY, Hamburg*

J. Weaver

*Synchrotron Radiation Center  
University of Wisconsin  
Stoughton, Wisconsin 53589, USA*



DESY behält sich alle Rechte für den Fall der Schutzrechtserteilung und für die wirtschaftliche Verwertung der in diesem Bericht enthaltenen Informationen vor.

DESY reserves all rights for commercial use of information included in this report, especially in case of apply for or grant of patents.

To be sure that your preprints are promptly included in the  
HIGH ENERGY PHYSICS INDEX ,  
send them to the following address ( if possible by air mail ) :

DESY  
Bibliothek  
Notkestrasse 85  
2 Hamburg 52  
Germany

The Influence of Intershell Interaction on the 3d and 5d Branching Ratio  
of Cu and Au<sup>+</sup>

J. Barth, R. Bruhn and B. Sonntag

II. Institut für Experimentalphysik der Universität Hamburg und  
Deutsches Elektronen-Synchrotron DESY, Hamburg

and J. Weaver

Synchrotron Radiation Center, University of Wisconsin, Stoughton,  
Wisconsin 53589, USA

A b s t r a c t

*The intensity ratio of the photoelectrons emitted from the upper and the lower parts of the d bands of polycrystalline Cu and Au films has been determined in the photon energy range from 40 eV to 120 eV. Intershell interaction gives rise to a significant increase of this ratio at the Cu 3p and Au 5p threshold.*

We report photoemission measurements on Cu and Au films evaporated under UHV conditions onto stainless steel substrates. Synchrotron radiation of the storage ring Tantalus I was monochromatized by a Grasshopper monochromator (1). The photoelectrons were analysed by a double path cylindrical mirror analyser whose axis was tilted by  $45^\circ$  against the sample surface normal. The samples were illuminated under  $20^\circ$  by s-polarized light. With respect to the axis of the analyser the collection geometry corresponds to averaging over all azimuthal angles and polar angles between  $36^\circ$  and  $48^\circ$ .

Energy distribution curves (EDC's) for photon energies between 40 eV and 120 eV were taken with an overall resolution of 0.4 eV in steps of 1 eV. The EDC's were corrected for the spectral output of the monochromator, the variation of the current in the storage ring and the analyser efficiency. The analyser efficiency was assumed to be proportional to the ratio of the pass energy  $E_p$  (25 eV) to the kinetic energy  $E_k$  (2, 3). Secondary electron background determined by interpolation has been subtracted. Fig. 1 shows typical EDC's for Cu and Au.

<sup>+</sup> to be published in Physics Lett. A



### Experimental Results

Au: The relative total valence band cross-section of Au extracted from a series of EDC's is presented in Fig. 2. The valence band states mainly stem from the atomic 5d levels. In agreement with the calculated atomic 5d cross section (4, 5) the total valence band cross-section decreases with increasing photon energy. Our results are in qualitative agreement with previously published results (6, 7). The slope of our results being steeper than reported previously is in better agreement with the theory (4, 5). For a more detailed analysis the energy dependence of the electron escape depth (8) and refraction effects, neglected in the analysis of the experimental data presented so far, have to be taken into account (9). In contrast to the theory (4, 5) there are additional features in the cross-sections, a maximum at 45 eV, a doublet centered at 65 eV and shoulders at  $\sim 80$  eV. These structures have their counterparts in the Au absorption spectrum (10). The relative cross-section of the upper part UP and the lower part LP (see Fig. 1) of the valence band, also given in Fig. 2, differ considerably. The maximum at 45 eV in the UP curve shows up at 47 eV in the LP curve indicating that it is mainly due to final state effects. The UP curve shows a prominent double peak at 62 eV and 67 eV and two shoulders at 79 eV and 85 eV, whereas corresponding structures are hardly discernible in the LP curve. At 50 eV both curves almost coincide. Above 50 eV they separate, the UP values being considerably higher than the LP values. The curves start to approach each other for photon energies above 85 eV. This behavior is reflected by the ratio of the UP to the LP cross-section, which goes through a minimum at 50 eV, reaches a maximum at 85 eV and decreases towards still higher energies. The monotonous rise between these energies is interrupted by a step at  $\sim 70$  eV. This result is in qualitative agreement with the ratio between the amplitude of the upper and the lower valence band maximum obtained by Barth (11) from published photoemission data.

Cu: The relative total valence band cross-section of Cu is presented in Fig. 3. The maximum at 47 eV is followed by a decline towards higher energies. The most interesting feature is the marked depression at the 3p threshold at 75 eV. The energy dependence of the amplitude ratio between the upper (B) and the lower (A) valence band peak (see Fig. 1) is similar to the corresponding curve for Au. The ratio goes through a minimum near 60 eV and peaks at 80 eV. There is also an indication of a step at  $\sim 75$  eV, though the step is far less pronounced than in Au.

### Discussion

Considerable variations of the relative peak heights of the valence band maxima have been observed in angle resolved photoemission measurements on different faces of Cu and Au single crystals (6). These variations have been discussed in terms of transitions between the d valence bands and high lying conduction bands, i.e. in terms of electron band structure. Due to the strong dependence on the crystal orientation most of these variations are averaged out in angle integrated measurements on polycrystalline samples. This is borne out by the smooth, atomic-like behavior of subshell cross-sections determined this way (3, 6, 7, 8). The ratio of the two valence band maxima starts to rise right at the Au 5p and the Cu 3p threshold (see Figs. 2, 3). For Au the spin-orbit splitting of the  $5p_{1/2}$  and  $5p_{3/2}$  levels is well reproduced by the stepwise ascent. Even for Cu there is a weak indication of the spin-orbit splitting of the  $3p_{1/2}$ ,  $3p_{3/2}$  levels. This coincidence strongly favors an interpretation in terms of an interaction between the Au  $5p \rightarrow d$  and  $5d \rightarrow f$  and the Cu  $3p \rightarrow d$  and  $3d \rightarrow f$  excitations. Here d(f) stands for d(f)-symmetric continuum orbitals. In a simple approach this interaction can be visualized as a 5p (3p) excitation which decays via recombination thereby exciting a 5d (3d) valence electron. The final state reached this way is indistinguishable from the state reached by direct valence band photoemission. For atomic and solid transition metals this type of intershell interactions has been clearly verified (see e.g. Refs. 3, 12). The neglect of the  $p \rightarrow s$  and  $d \rightarrow p$  transitions is justified by their small oscillator strength in this energy range compared to the  $p \rightarrow d$  and  $d \rightarrow f$  transitions. The small oscillator strength of the Au 4f transitions at threshold (4, 5) explains the absence of any noticeable change of the UP versus the LP ratio at the Au 4f threshold. It is interesting to note that the increase of the amplitude ratio of the two Au valence band maxima above 140 eV reported by Lindau et al. (8) closely follows the rise of the 4f cross-section (4, 5, 8). It appears reasonable to attribute this ratio increase to the interaction between the  $4f \rightarrow g$  and  $5d \rightarrow f$  excitations. Thus the prominent features in the amplitude ratio of the two valence band maxima for Cu and Au can be explained in a consistent way by taking intershell correlation into account.

The ratio of the two valence band maxima is related to the atomic  $\sigma_{d5/2}/\sigma_{d3/2}$  branching ratio, in case the spin-orbit projected densities of states show

more  $d_{5/2}$  character in the upper and more  $d_{3/2}$  character in the lower part of the valence band. For Au the spin orbit-splitting of the Au  $5d_{3/2}$ ,  $5d_{5/2}$  levels is of the same order of magnitude as the separation of the two valence band peaks. The upper valence band maximum contains more states of  $5d_{5/2}$  character, the lower maximum more states of  $5d_{3/2}$  character (13). This strongly favors the interpretation in terms of the atomic 5d branching ratio. Atomic branching ratios can deviate considerably from the statistical ratio  $l + 1/l$ . In many cases these deviations can be explained without taking correlation effects into account (14). This approach fails to explain the variation of the "branching ratio" of Au and Cu in the energy range between 50 eV and 110 eV. For atomic rare gases Johnson and Cheng (13) have proven how dramatically the branching ratios  $^2P_{3/2} : ^2P_{1/2}$  of the outer p shells are modified by intershell correlations. For Kr and Xe the interaction with excitations from the Kr 3d and Xe 4d shell gives rise to a significant increase of the branching ratio in the region of the inner shell threshold. The essence of this atomic model for the energy dependence of the branching ratio can be transferred to the solids in case interactions with inner shell excitations are involved. The atomic character of inner shells (Cu 3p, Au 5p) is preserved in the metals. The outer d-states are modified in the metals but still exhibit a strongly localized character. From total and partial cross-sections we know that the final state wavefunctions 30 eV above  $E_F$  can be approximated by atomic continuum functions in the region close to the nucleus, i.e. in the region of overlap with the core states (16).

#### Figure Captions

- Fig. 1 Representative EDC's for Cu and Au. The dashed areas give the valence band photoemission corrected for secondary electron background. The position of the two Cu valence band maxima A and B is indicated. The Au EDC's show the separation of the valence band into an upper part UP and a lower part LP.
- Fig. 2 Total relative Au valence band cross-section ( $\sigma_{5d}$ ) and relative cross-section of the upper ( $\sigma_{UP}$ ) and the lower part ( $\sigma_{LP}$ ) of the valence band. The ratio  $\sigma_{UP}/\sigma_{LP}$  is given by the dashed line. The binding energies of the core levels have been taken from Ref. 17.
- Fig. 3 Total relative Cu-valence band cross-section  $\sigma_{3d}$ . The amplitude ratio B/A of the two valence band maxima is given by the dashed line. The binding energies of the core levels have been taken from Ref. 17.

## References

- (1) F.C. Brown, R.Z. Bachrach and N. Lien, Nucl. Instr. and Methods 152 (1978) 73
- (2) P.W. Palmberg, J. Electron Spectr. and Related Phenomena 5 (1974) 691
- (3) J. Barth, F. Gerken, K.L.I. Kobayashi, J.H. Weaver and B. Sonntag, J. Phys. C13 (1980) 1369
- (4) S.T. Manson and J.W. Cooper, Phys. Rev. 165 (1968) 126
- (5) F. Combet Farnoux and Y. Héno, Compt. Rend. 264B (1967) 138
- (6) J. Stöhr, G. Apai, P.S. Wehner, F.R. McFeely, R.S. Williams and D.A. Shirley, Phys. Rev. B14 (1976) 5144
- (7) L.I. Johansson, I. Lindau, M. Hecht, S.M. Goldberg and C.S. Fadley, Phys. Rev. B20 (1979) 4126
- (8) I. Lindau and W.E. Spicer, J. Electron Spectrosc. Relat. Phenom. 3 (1974) 409
- (9) L.I. Johansson, M.H. Hecht and I. Lindau, J. Electron Spectrosc. Relat. Phenom. 18 (1980) 271
- (10) H.I. Hagemann, W. Gudat and C. Kunz, J. Opt. Soc. Am. 65 (1975) 742
- (11) J. Barth, DESY Rep. SR-79/32
- (12) R. Bruhn, B. Sonntag and H.W. Wolff, J. Phys. B12 (1979) 203
- (13) N.E. Christensen, J. Phys. F 8 (1978) L51
- (14) T.E.H. Walker and J.T. Waber, J. Phys. B 7 (1974) 674
- (15) W.R. Johnson and K.T. Cheng, Phys. Rev. A20 (1979) 978
- (16) see e.g. B.F. Sonntag, J. de Physique 39 (1978) C4
- (17) M. Cardona and L. Ley, in Photoemission in Solids I, Topics in Applied Physics, Vol. 26 (1978) 265

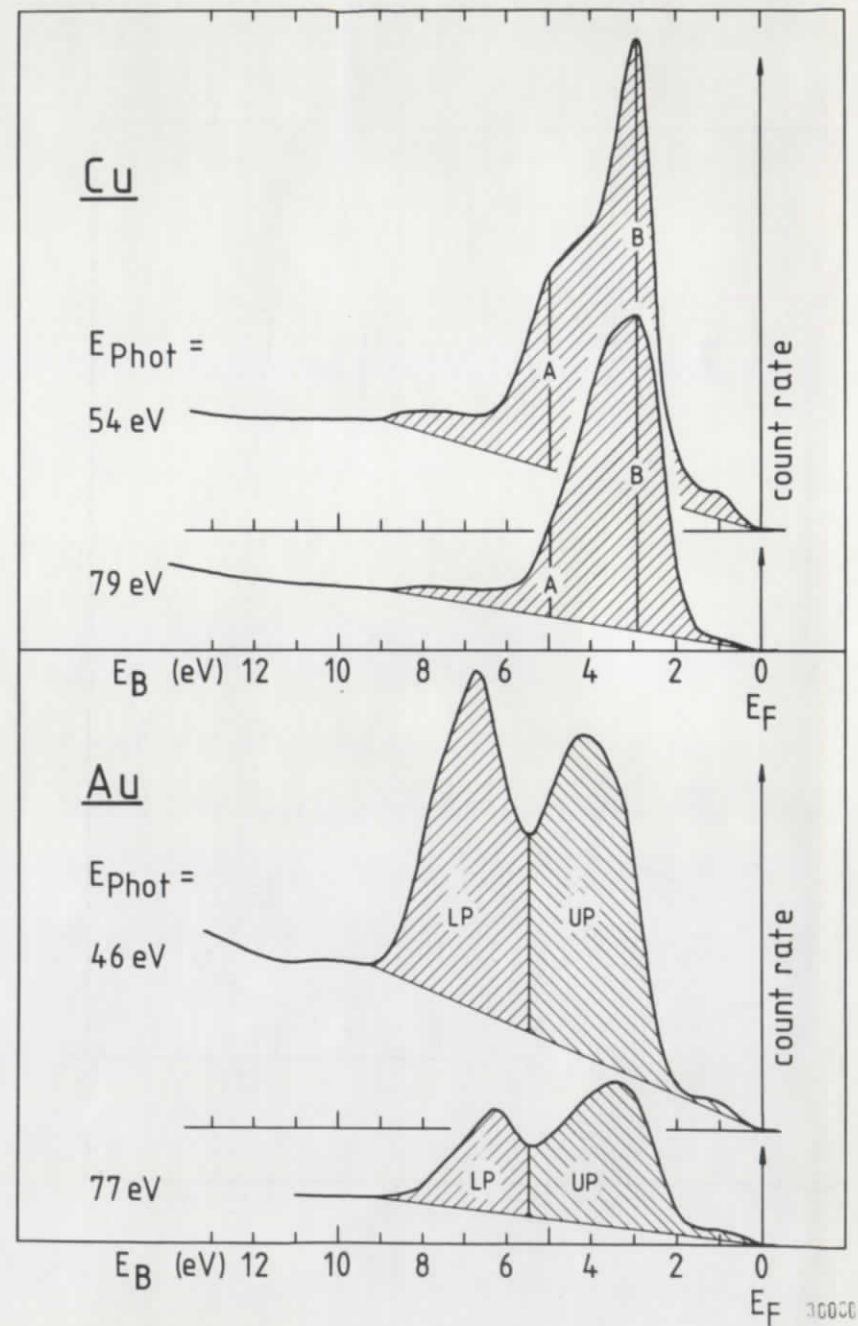


Fig. 1

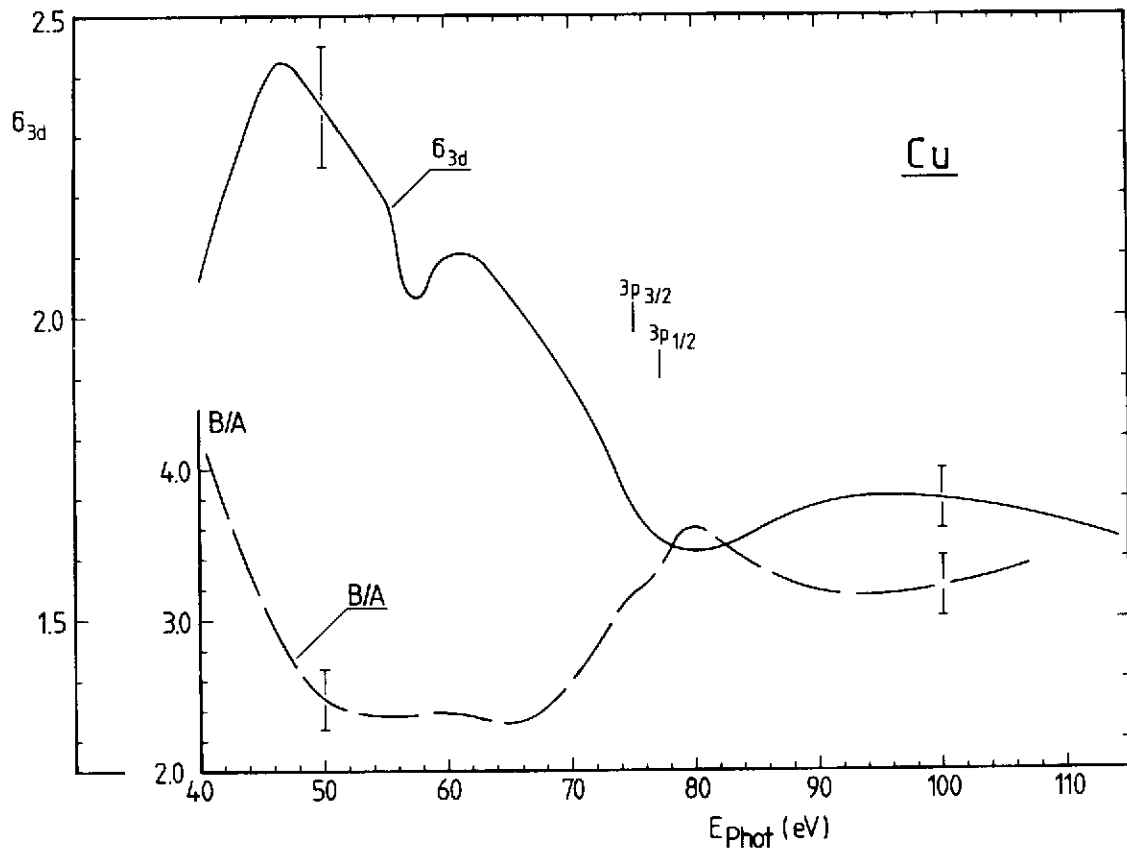


Fig. 3

2926

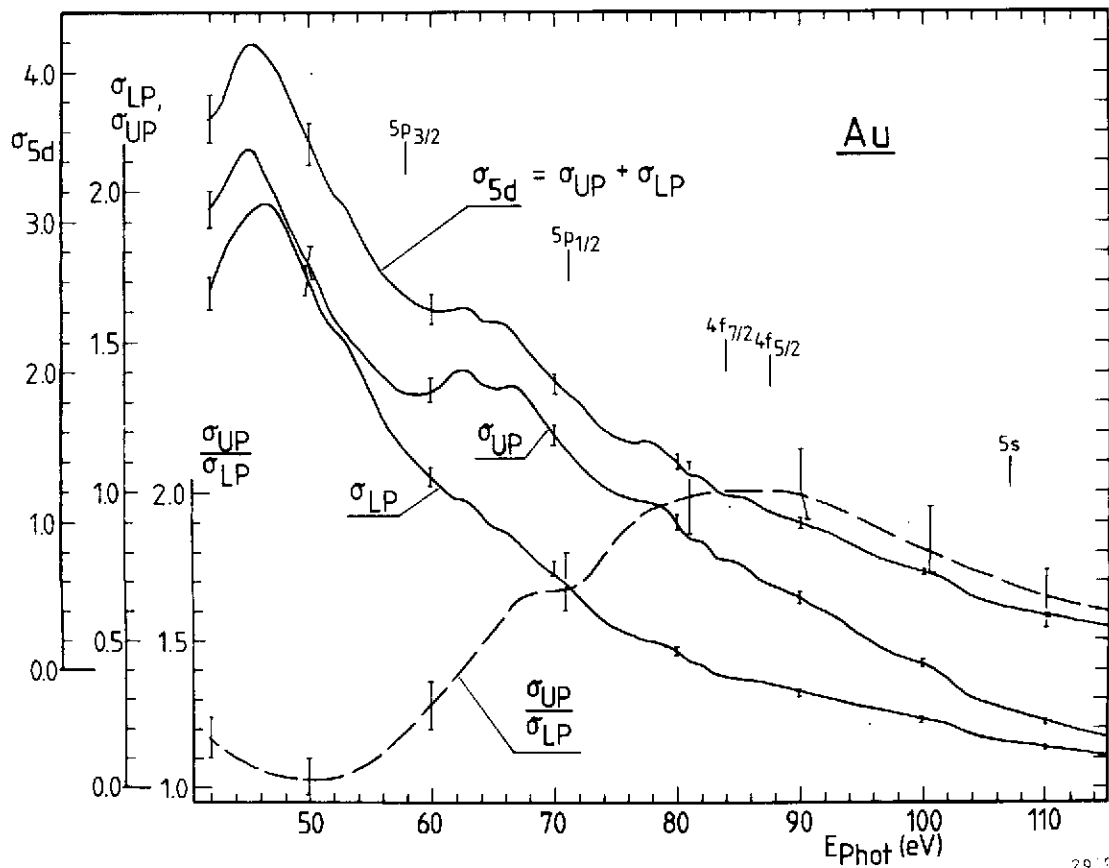


Fig. 2

2928